

# Fractional model for CoViD-19 dynamics

João P. S. Maurício de Carvalho<sup>\*a</sup> and Beatriz Moreira-Pinto<sup>b</sup>

<sup>a</sup>Faculty of Sciences, University of Porto,  
Rua do Campo Alegre s/n, 4169-007 Porto, Portugal  
*up200902671@fc.up.pt*

<sup>b</sup>UCIBIO, REQUIMTE, Faculty of Pharmacy, University of Porto  
Rua de Jorge Viterdo Ferreira, 228, 4050-313 Porto, Portugal  
*abeatriz\_pinto@hotmail.com*

---

## Abstract

Coronavirus disease 2019 (CoViD-19) is an infectious disease caused by severe acute respiratory syndrome coronavirus 2 (SARS-CoV-2). Among many symptoms, cough, fever and tiredness are the most common. People over 60 years old and with associated comorbidities are most likely to develop a worsening health condition. In this paper is proposed a non-integer order model to describe the dynamics of CoViD-19 in a standard population. The model incorporates the reinfection rate in the individuals recovered from the disease. Numerical simulations of the model are performed for different values of the order of the fractional derivative and for different values of reinfection rate. The results are discussed from a biological point of view.

*Keywords:* COVID-19, mathematical model, epidemic model, reinfection, fractional calculus

---

## 1. Introduction

At the end of the year 2019, a newly discovered coronavirus named Severe Acute Respiratory Syndrome Coronavirus 2 (SARS-CoV-2) emerged in Wuhan, China [1]. The disease was later designated by the World Health Organization (WHO) as Coronavirus Disease 2019 or CoViD-19. CoViD-19

---

\* corresponding author

has demonstrated a great capacity of propagation directly through human-to-human contact and the epidemic quickly began to spread on a worldwide level, claiming multiple lives throughout its course [2]. At the time of writing, according to the reports of WHO, CoViD-19 pandemic has caused 2 217 005 deaths out of a total of 102 399 513 people infected [3]. Clinical manifestations can range from asymptomatic to symptoms that include high fever, dry cough, lack of smell and/or taste, shortness of breath for mild cases and pneumonia for severe cases [4]. However, the severity of the disease may vary depending on age (i.e., 65 years old or more) and pre-existing conditions such as diabetes, obesity, hypertension and other conditions that compromise the immune system [5]. Several studies have also reported neuronal, gastrointestinal, cardiological and long-term pulmonary complications [6, 7, 8].

With the accelerated growth in the number of cases and deaths, a combination of public health measures has been recommended to mitigate the spread of the virus and avoid overloading health systems. Thus, several measures had to be imposed by the governments to try to control and prevent the possibility of contagion. Some of them include isolation of confirmed cases and quarantine of the suspected ones, implementation of community lockdown, closing borders, maintaining social distancing and the use of face masks [9].

Several mathematical models have been proposed to understand the dynamics of CoViD-19, being extremely useful to understand the mechanism of transmission, as well as, to predict the future behavior of the disease and control possible outbreaks [10, 11, 12]. Çakan [13] proposed a mathematical SEIR epidemic model (susceptible – exposed – infected – recovered) to evaluate the impact of CoViD-19 in the hospital environment. It was possible to conclude that an increase in contact rates between susceptible and infected individuals may lead to a breakdown in hospitals and deplete their resources. Buonomo [14] proposed a mathematical SIRI model (susceptible – infected – recovered – infected) to analyse the effects of a vaccine on a population where CoViD-19 was predominant. The author concluded that the incidence of the disease can be reduced by increasing the information given to the population and/or when the information delay is short, particularly when the rate of reinfection in the community is high. Khoshnaw *et al.* [15] developed some existing mathematical models and made a new numerical analysis of them. In addition, they studied the sensitivity of important parameters in the reproduction number variation. The results show that the

contact rate, the exposure rate during quarantine and the transition rate of exposed individuals play a key role in the spread of the disease.

### *Fractional calculus*

The literature on fractional calculus (FC) applications has grown significantly in recent times. Some relevant articles can be found in the area of engineering, physics, biology, epidemiology, finance, among others [16]. Ahmad *et al.* [17] presented a non-integer derivative model for the transmission of CoViD-19. They showed that as the order of the fractional order (FO) derivative increases the solution approaches to the result at integer order 1. After comparing the simulations for different values of the FO derivative they found that the simulated curve that most closely approximates the real curve happens for  $\alpha = 0.97$ . Zhang *et al.* [18] developed a non-integer order model for the CoViD-19 dynamics. They analysed the reproduction number and investigated the asymptotic stability of the model. They applied the adaptive predictor-corrector algorithm and fourth-order Runge-Kutta method to simulate it. The numerical results showed firm agreement with the theoretical results.

These models inspired us to formulate a FO mathematical model for population dynamics in the presence of CoViD-19. The purpose of this study is to analyse the impact of isolation, reinfection and recovery rates of individuals in the population due to the presence of the disease in the community. In Section 2 we describe the model and prove that it is positive and bounded. In Section 3 we calculate the basic reproduction number, study the stability around the disease-free equilibrium point and perform the sensitivity analysis of relevant parameters in the spread of CoViD-19. In Section 4 we simulate the model for all relevant parameters and we comment on their results. We draw some conclusions and present future work in Section 5.

## **2. Model interpretation**

Four classes of individuals incorporate the model: susceptible,  $S(t)$ , infected,  $I(t)$ , isolated/quarantined,  $Q(t)$ , and recovered,  $R(t)$ . With respect to our model, we define  $\Omega = \{(\lambda, \beta, \mu, r, \sigma, \theta) \in (\mathbb{R}^+)^6\}$  as the set of parameters. The recruitment rate of susceptible individuals is given by  $\lambda^\alpha$ . The contact rate of susceptible and recovered individuals with infected population is given by  $\beta^\alpha$ , then they move into the class of infected individuals. The term  $\sigma^\alpha I$

represents the fraction of infected individuals who became isolated. Isolated individuals recover from the disease at a rate  $\theta^\alpha$ . The susceptibility of an individual who has recovered from the disease to becoming infected again is given by  $p^\alpha$ . So, it makes sense to consider that  $r^\alpha = \beta^\alpha p^\alpha$  is the reinfection rate of individuals who have already recovered from the disease. Parameters  $\mu_S^\alpha$ ,  $\mu_I^\alpha$ ,  $\mu_Q^\alpha$  and  $\mu_R^\alpha$  are the natural death rates of susceptible, exposed, infected, isolated and recovered individuals, respectively. It is assumed an equal value for every natural death rates to simplify algebraic calculations in this paper, i.e,  $\mu_S^\alpha = \mu_I^\alpha = \mu_Q^\alpha = \mu_R^\alpha \equiv \mu^\alpha$ .

A description of the model variables and all parameters can be found in Table 1. The nonlinear system of FO equations is given by

$$\begin{aligned}
\frac{d^\alpha S}{dt^\alpha} &= \lambda^\alpha - \beta^\alpha SI - \mu^\alpha S \\
\frac{d^\alpha I}{dt^\alpha} &= \beta^\alpha SI + r^\alpha RI - \sigma^\alpha I - \mu^\alpha I \\
\frac{d^\alpha Q}{dt^\alpha} &= \sigma^\alpha I - \theta^\alpha Q - \mu^\alpha Q \\
\frac{d^\alpha R}{dt^\alpha} &= \theta^\alpha Q - r^\alpha RI - \mu^\alpha R,
\end{aligned} \tag{1}$$

where  $\alpha \in (0, 1]$  is the order of the fractional derivative. We use the concept of a FO derivative proposed by Caputo:

$$\frac{d^\alpha y(t)}{dt^\alpha} = I^{p-\alpha} y^{(p)}(t), \quad t > 0, \tag{2}$$

where  $p = [\alpha]$  is the integer part of  $\alpha$ ,  $y^{(p)}$  is the  $p$ -th derivative of  $y(t)$  and  $I^{p_1}$  is the Riemann-Liouville fractional integral

$$I^{p_1} z(t) = \frac{1}{\Gamma(p_1)} \int_0^t (t-t')^{p_1-1} z(t') dt'. \tag{3}$$

### 2.1. Model properties analysis

The solutions of the system (1) remain non-negative for the entire domain,  $t > 0$ . Let  $R_+^4 = \{x \in R^4 \mid x \geq 0\}$  and  $x(t) = (S(t), I(t), Q(t), R(t))^T$ . First, we quote the following Generalized Mean Value Theorem [19] and corollary.

Variable	Symbol
Susceptible population	$S(t)$
Infected population	$I(t)$
Isolated population	$Q(t)$
Recovered population	$R(t)$

Table 1: Description of the variables of model (1).

**Lemma 1.** [19] Suppose that  $f(x) \in C[a, b]$  and  $D_a^\alpha f(x) \in C(a, b)$ , where  $0 < \alpha \leq 1$ , thus

$$f(x) = f(a) + \frac{1}{\Gamma(\alpha)} (D_a^\alpha f)(\xi) \cdot (x - a)^\alpha \quad (4)$$

for  $a \leq \xi \leq x, \forall x \in (a, b]$  and  $\Gamma(\cdot)$  is the gamma function.

**Corollary 1.** Let  $f(x) \in C[a, b]$  and  $D_a^\alpha f(x) \in C(a, b)$ , for  $0 < \alpha \leq 1$ .

1. If  $D_a^\alpha f(x) \geq 0, \forall x \in (a, b)$ , then  $f(x)$  is non-decreasing for each  $x \in [a, b]$ ;
2. If  $D_a^\alpha f(x) \leq 0, \forall x \in (a, b)$ , then  $f(x)$  is non-increasing for each  $x \in [a, b]$ .

This proves the main theorem.

**Theorem 2.** There is a unique solution  $x(t) = (S(t), I(t), Q(t), R(t))^T$  to the system (1) in the entire domain ( $t \geq 0$ ). Furthermore, the solution remains in  $R_+^4$ .

**Proof.**

As we can see from Theorem 3.1 and Remark 3.2 of [20], the solution of the initial value problem exists and is unique, for  $t \geq 0$ . Then, it is enough to prove that the non-negative orthant  $R_+^4$  is positively invariant. So, we must demonstrate that the vector field points to  $R_+^4$  in each hyperplane, thus limiting the non-negative orthant. Hence, we have:

$$\begin{aligned}
\frac{d^\alpha S}{dt^\alpha} \Big|_{S=0} &= \lambda^\alpha \geq 0 \\
\frac{d^\alpha I}{dt^\alpha} \Big|_{I=0} &= 0 \\
\frac{d^\alpha Q}{dt^\alpha} \Big|_{Q=0} &= \sigma^\alpha I \geq 0 \\
\frac{d^\alpha R}{dt^\alpha} \Big|_{R=0} &= \theta^\alpha Q \geq 0.
\end{aligned} \tag{5}$$

According to the Corollary 1, it can be concluded that the solution remains in  $R_+^4$ .

### 3. Reproduction number and disease-free equilibria

In this section we compute the reproduction number,  $\mathcal{R}_0$  of the model (1). Basic reproduction number is the number of secondary infections caused by a single infected person in a susceptible population [21].

A disease-free equilibrium of the model (1) is obtain via imposing  $I = Q = R = 0$ .

$$\begin{aligned}
E^* &= (S^*, I^*, Q^*, R^*) \\
&= \left( \frac{\lambda^\alpha}{\mu^\alpha}, 0, 0, 0 \right)
\end{aligned}$$

Using Lemma 1 of [21] in system (1), the matrices for the new infection terms,  $F$ , and the remaining terms,  $V$ , are the following:

$$\begin{aligned}
F &= \begin{pmatrix} \beta^\alpha S^* + r^\alpha R^* & \beta^\alpha I^* \\ 0 & 0 \end{pmatrix} \\
V &= \begin{pmatrix} \sigma^\alpha + \mu^\alpha & 0 \\ \beta^\alpha S^* & \beta^\alpha I^* + \mu^\alpha \end{pmatrix}
\end{aligned} \tag{6}$$

and the associative basic reproduction number is given by:

$$\mathcal{R}_0 = \rho(FV^{-1}) = \frac{\beta^\alpha \lambda^\alpha}{\mu^\alpha (\sigma^\alpha + \mu^\alpha)} \quad (7)$$

where  $\rho$  is the spectral radius of the matrix  $FV^{-1}$ .  
By Theorem 2 of [21] we obtain the Lemma 3.

**Lemma 3.** *The disease-free equilibrium  $E_0$  is locally asymptotically stable if  $\mathcal{R}_0 < 1$  and unstable if  $\mathcal{R}_0 > 1$ .*

**Proof.** Let

$$L(E^*) = \begin{pmatrix} -\mu^\alpha & -\frac{\beta^\alpha \lambda^\alpha}{\mu} & 0 & 0 \\ 0 & \frac{\beta^\alpha \lambda^\alpha}{\mu^\alpha} - \sigma^\alpha - \mu^\alpha & 0 & 0 \\ 0 & \sigma^\alpha & -\theta^\alpha - \mu^\alpha & 0 \\ 0 & 0 & 0 & -\mu^\alpha \end{pmatrix} \quad (8)$$

be the matrix of linearization of the model (1) around de disease-free equilibrium,  $E^*$ . The eigenvalues of  $L(E^*)$  are given by:

$$\begin{aligned} \lambda_1 &= -\theta^\alpha - \mu^\alpha \\ \lambda_2 &= \frac{\beta^\alpha \lambda^\alpha - \mu^{\alpha 2} - \mu^\alpha \sigma^\alpha}{\mu^\alpha} \\ \lambda_3 &= \lambda_4 = -\mu^\alpha. \end{aligned} \quad (9)$$

It is easy to verify that the eigenvalues  $\lambda_1$ ,  $\lambda_3$  and  $\lambda_4$  have negative real part. With regard to  $\lambda_2$ , there is a negative real part if

$$\begin{aligned}
& \lambda_2 < 0 \\
& \Leftrightarrow \frac{\beta^\alpha \lambda^\alpha - \mu^{\alpha 2} - \mu^\alpha \sigma^\alpha}{\mu^\alpha} < 0 \\
& \Leftrightarrow \beta^\alpha \lambda^\alpha - \mu^{\alpha 2} - \mu^\alpha \sigma^\alpha < 0 \\
& \Leftrightarrow \beta^\alpha \lambda^\alpha < \mu^\alpha (\sigma^\alpha + \mu^\alpha) \\
& \Leftrightarrow \frac{\beta^\alpha \lambda^\alpha}{\mu^\alpha (\sigma^\alpha + \mu^\alpha)} < 1 \\
& \stackrel{(7)}{\Leftrightarrow} \mathcal{R}_0 < 1.
\end{aligned}$$

Thus, if  $\mathcal{R}_0 < 1$ , then all eigenvalues have a negative real part. Therefore  $E^*$  is locally asymptotically stable under this condition. On the other hand, if

$$\begin{aligned}
& \lambda_2 > 0 \\
& \Leftrightarrow \frac{\beta^\alpha \lambda^\alpha - \mu^{\alpha 2} - \mu^\alpha \sigma^\alpha}{\mu^\alpha} > 0 \\
& \Leftrightarrow \beta^\alpha \lambda^\alpha - \mu^{\alpha 2} - \mu^\alpha \sigma^\alpha > 0 \\
& \Leftrightarrow \beta^\alpha \lambda^\alpha > \mu^\alpha (\sigma^\alpha + \mu^\alpha) \\
& \Leftrightarrow \frac{\beta^\alpha \lambda^\alpha}{\mu^\alpha (\sigma^\alpha + \mu^\alpha)} > 1 \\
& \stackrel{(7)}{\Leftrightarrow} \mathcal{R}_0 > 1.
\end{aligned}$$

So, if  $\mathcal{R}_0 > 1$  then  $\lambda_2 > 0$ . Therefore  $E^*$  is unstable.



### 3.1. Sensitivity analysis

Sensitivity indices allow us to have a perspective on the relative change of a variable when a parameter varies. This sensitivity index is the ratio between the relative change in the variable and the relative change in the parameter. When the variable,  $v$ , is a differentiable function of these parameters,  $p$ , the sensitivity index can be calculated through partial derivatives, using the following expression [22]:

$$\gamma_p^v = \frac{\partial v}{\partial p} \times \frac{p}{v}. \quad (10)$$

In the case of  $\mathcal{R}_0$ , comes that

$$\gamma_p^{\mathcal{R}_0} = \frac{\partial \mathcal{R}_0}{\partial p} \times \frac{p}{\mathcal{R}_0} \quad (11)$$

and the sign of the sensitivity indices corresponding to the basic reproduction number is given in Table 2. The sensitivity indices signs give us information about the variation of the value of  $\mathcal{R}_0$ .

Index	Sensitivity index sign
$\gamma_{\lambda^\alpha}^{\mathcal{R}_0}$	+1.00
$\gamma_{\beta^\alpha}^{\mathcal{R}_0}$	+1.00
$\gamma_{\sigma^\alpha}^{\mathcal{R}_0}$	-0.98

Table 2: Sensitivity indices for relevant parameters of model (1)

Table 2 shows that the parameter  $\lambda^\alpha$  and  $\beta^\alpha$  contribute to the spread of the disease. This means that when the value of recruitment rate and the value of contact rate between susceptible and recovered with infected individuals increases, the number of infected people also increases. The magnitude of  $\lambda^\alpha$  and  $\beta^\alpha$  is positive and of equal value. On the other hand, it is observed that the rate at which infected people are quarantined,  $\sigma^\alpha$ , has an opposite effect. Thus, the isolation rate slows the spread of the disease.

#### 4. Numerical results

In this section it is simulated the system (1). The parameter values used in the numerical simulations are in Table 3 and the initial conditions are  $S(0) = 153$ ,  $I(0) = 138$ ,  $Q(0) = 68$  and  $R(0) = 20$  [18].

Parameter	Symbol	Value	Reference
Recruitment rate of susceptible individuals	$\lambda^\alpha$	$1.45 \times 10^{-1}$	[18]
Contact rate with infected individuals	$\beta^\alpha$	$3.80 \times 10^{-4}$	[18]
Isolation rate of infected individuals	$\sigma^\alpha$	$1.69 \times 10^{-2}$	[18]
Recovery rate of isolated individuals	$\theta^\alpha$	$1.81 \times 10^{-2}$	[18]
Susceptibility due to previous infection	$p^\alpha$	$[0, 1)$	[14]
Natural death rate of individuals	$\mu^\alpha$	$4.10 \times 10^{-4}$	[18]
Reinfection rate of recovered individuals	$r^\alpha$	$[0, 3.80 \times 10^{-4})$	[14]

Table 3: Parameter values used in numerical simulations of model (1)

Figure 1 shows the behaviour of population classes of model (1) for  $\alpha = 1$ . Over time, it is perceived that the density of infected people reaches its peak (around 200 people) after approximately 25 days. However, the number of infected individuals tends to decrease to less than 100. One of the factors that can influence this decrease may be the increase in the number of isolated and recovered people.

In Figure 2, the dynamics of infected and isolated individuals were simulated for three isolation rates,  $\sigma^\alpha$ , considering different  $\alpha$  values. In the first days it is observed that the number of infected people drops with the increase of isolated ones. Moreover, the higher the isolation rate, the greater the decrease of infected individuals. The number of CoViD-19 positive is controlled through the isolation of the confirmed cases, preventing the spread of the disease. This causes the number of infected people to decrease over time. As a result, the number of isolated ones decreases slowly. This happens regardless of the value of  $\alpha$ . Furthermore, the lower the value of the order of the fractional derivative, the lower the number of infected people.

Figure 3 displays the behaviour of infected and isolated individuals considering three values of the reinfection rate,  $r^\alpha$ . The increase in the reinfection rate increases the number of people who are ill, no matter what the value of  $\alpha$  is. With the increase of infected individuals the number of people who become isolated also increases. This behaviour is independent of the value

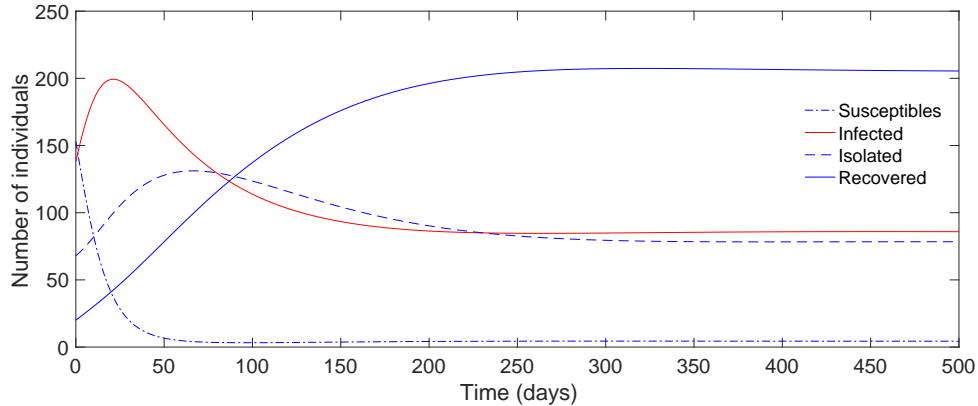


Figure 1: Dynamics of model (1)

of the derivative of FO. In addition, the lower the value of  $\alpha$  the lower the number of sick people and people in isolation.

Figure 4 describes the density of infected and recovered individuals in the first 1000 days, for different combinations of isolation and recovery rates,  $\sigma^\alpha$  and  $\theta^\alpha$  respectively, and  $\alpha = 1$ . On the left, low recovery rate promotes a high number of CoViD-19 patients (around 350 people). In general, high values of  $\theta^\alpha$  mean fewer people are infected. On the right, very high recovery rates combined with values greater than about  $10^{-2}$  of isolation rate promotes a relatively high number of people recovered from the disease (greater than 140 people).

## 5. Conclusion

In this work, a FO model for the dynamics of a population in the presence of CoViD-19 was formulated and analyzed.

From a theoretical point of view, the reproduction number around the disease-free equilibrium point was calculated and the impact that the parameters of the model have on it was discussed. Local stability around the disease-free equilibrium point was proven for  $\mathcal{R}_0 < 1$ .

From a numerical point of view the model was simulated for relevant parameters. The isolation of people with CoViD-19 causes a drop in the number of infected people. On the other hand, the decrease of the disease in the population leads to a reduced need for isolation. A decrease of the FO derivative,  $\alpha$ , results in fewer people being infected and isolated over

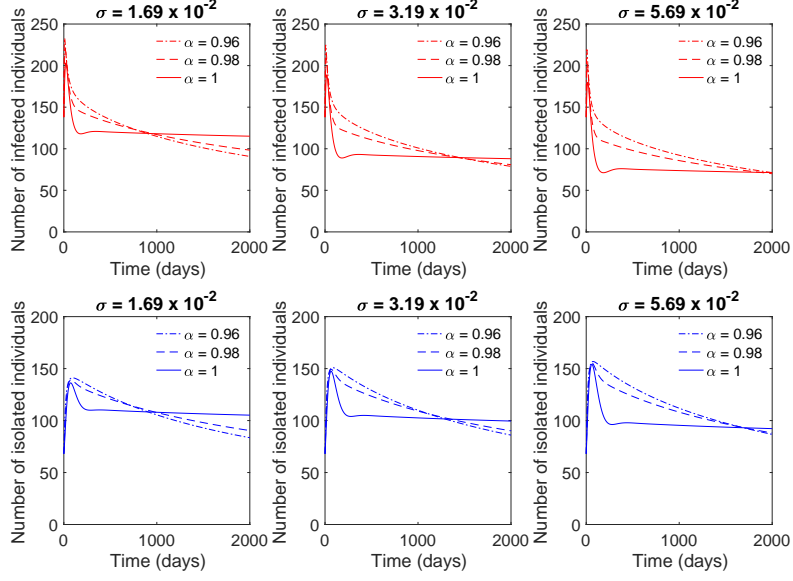


Figure 2: Dynamics of infected and isolated individuals for  $\sigma = \{1.69 \times 10^{-2}, 3.19 \times 10^{-2}, 5.69 \times 10^{-2}\}$ ,  $r = 0.30\beta$  and  $\alpha = \{0.96, 0.98, 1\}$

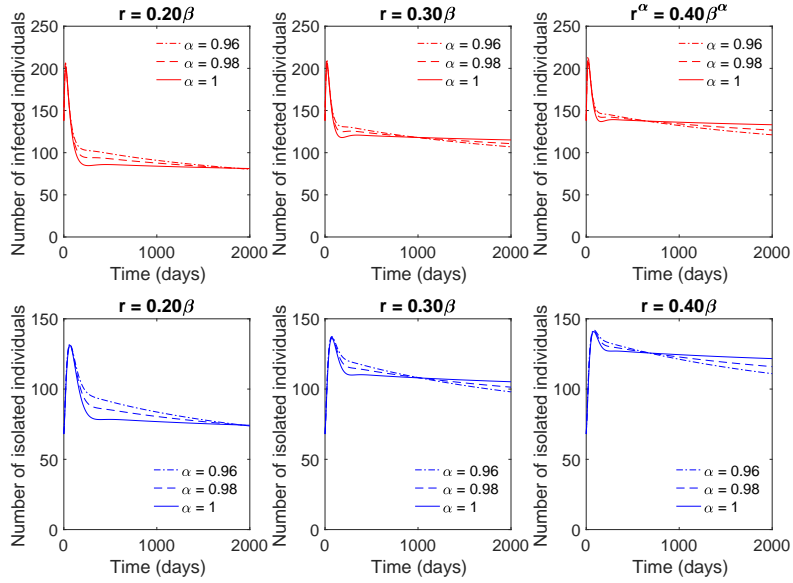


Figure 3: Dynamics of infected and isolated individuals for  $r = \{0.20\beta, 0.30\beta, 0.40\beta\}$  and  $\alpha = \{0.96, 0.98, 1\}$

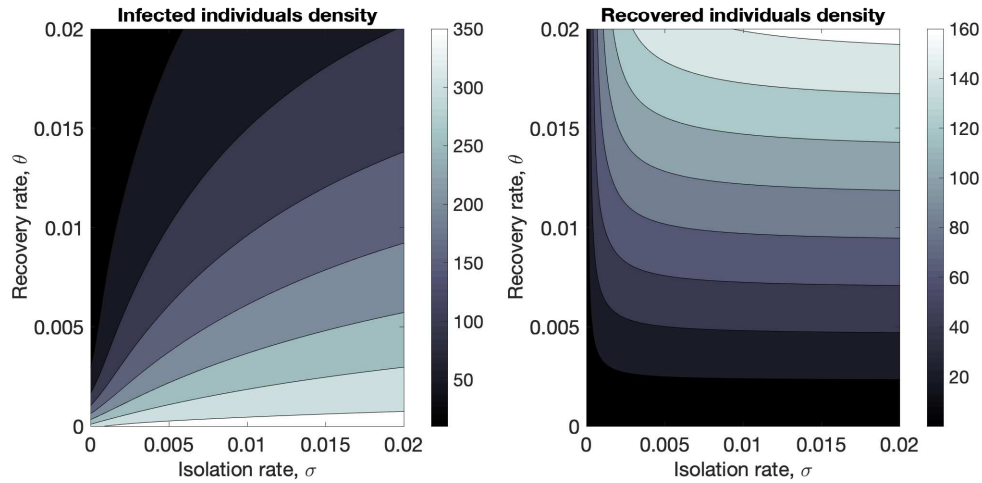


Figure 4: Infected (left) and recovered (right) individuals density after 1000 days, considering some combinations of isolation,  $\sigma$ , and recovered,  $\theta$ , rates, for  $\alpha = 1$

time. A greater susceptibility to a new infection increases the number of people infected and causes CoViD-19 to firmly persist in the population. So the higher the rate of reinfection in the population, the more people will become infected. Consequently, the number of people in quarantine will also increase. Low  $\alpha$  values induce fewer people with CoViD-19 and fewer people in isolation for any value of the reinfection rate. Moreover, a high recovery rate and an isolation rate above  $10^{-2}$  is reflected in a population with fewer patients CoViD-19. Furthermore, a population with few people recovered from the disease cannot reduce the number of infected individuals. Consequently the disease spreads faster in the population.

The model does not include the impact of vaccination on the population. In our future work we aim to study population dynamics in the presence of different levels of vaccine effectiveness for CoViD-19.

## References

## References

- [1] J. J. V. Bavel, K. Baicker., P. S. Boggio et al., Using social and behavioural science to support COVID-19 pandemic response, *Nature human behaviour* **4** (2020) 460–471.

- [2] T. L. Dao, and P. Gautret, Recurrence of SARS-CoV-2 viral RNA in recovered COVID-19 patients: a narrative review, *European Journal of Clinical Microbiology & Infectious Diseases* (2020) 1–13.
- [3] World Health Organization (WHO), <https://www.who.int/emergencies/diseases/novel-coronavirus-2019>. Accessed in February 1 2021
- [4] Y.-D. Li, W. -Y. Chi, J. -H. Su, L. Ferrall, C. -F. Hung and T. -C. Wu, Coronavirus vaccine development: from SARS and MERS to COVID-19, *Journal of Biomedical Science* **27** (2020) 1–23.
- [5] H. A. Rothan and S. N. Byrareddy, The epidemiology and pathogenesis of coronavirus disease (COVID-19) outbreak, *Journal of Autoimmunity* **109** (2020) 4 pages.
- [6] F. Bompard, H. Monnier, I. Saab et al., Pulmonary embolism in patients with COVID-19 pneumonia, *European Respiratory Journal* **56** (2020) 9 pages.
- [7] O. Rodriguez-Leor, B. Cid-Alvarez, S. Ojeda et al., Impact of the COVID-19 pandemic on interventional cardiology activity in Spain, *REC Interv Cardiol* **2** (2020) 82–89.
- [8] H. -Y. Wang, X. -L. Li, Z. -R. Yan et al., Potential neurological symptoms of COVID-19, *Therapeutic advances in neurological disorders* **13** (2020) 1–2.
- [9] Z. D. Berger, N. G. Evans, A. L. Phelan and R. D. Silverman, Covid-19: control measures must be equitable and inclusive, *British Medical Journal Publishing Group* **368** (2020) 1–2.
- [10] N. P. Jewell, J. A. Lewnard and B. L. Jewell, Predictive mathematical models of the COVID-19 pandemic: underlying principles and value of projections, *Jama* **323** (2020) 1893–1894.
- [11] D. M. Thomas, R. Sturdivant, N. V. Dhurandhar et al., A primer on COVID-19 Mathematical Models, *Obesity* **28** (2020) 1375–1377.
- [12] A. Zeb, E. Alzahrani, V. S. Erturk and G. Zaman, Mathematical model for coronavirus disease 2019 (COVID-19) containing isolation class, *BioMed research international* **2020** (2020) 7 pages.

- [13] S. Çakan, Dynamic analysis of a mathematical model with health care capacity for COVID-19 pandemic, *Chaos, Solitons & Fractals* **139** (2020) 8 pages.
- [14] B. Buonomo, Effects of information-dependent vaccination behavior on coronavirus outbreak: insights from a SIRI model, *Ricerche di Matematica* (2020), 1–17.
- [15] S. H. A. Khoshnaw, R. H. Salih and S. Sulaimany, Mathematical modelling for coronavirus disease (COVID-19) in predicting future behaviours and sensitivity analysis, *Mathematical Modelling of Natural Phenomena* **15** (2020) 13 pages.
- [16] S. Samko, A. Kilbas and O. Marichev, *Fractional Integrals and Derivatives: Theory and Applications*, Gordon and Breach Science Publishers (1993), London.
- [17] S. Ahmad, A. Ullah, Q. M. Al-Mdallal et al., Fractional order mathematical modeling of COVID-19 transmission, *Chaos, Solitons & Fractals* **139** (2020) 10 pages.
- [18] Z. Zhang, A. Zeb, O. F. Egbelowo and V. S. Erturk, Dynamics of a fractional order mathematical model for COVID-19 epidemic, *Advances in Difference Equations* **2020** (2020) 1–16.
- [19] Z. M. Odibat and N. T. Shawagfeh, Generalized Taylor’s formula, *Applied Mathematics and Computation*, **186** (2007) 286–293.
- [20] W. Lin, Global existence theory and chaos control of fractional differential equations, *Journal of Mathematical Analysis and Applications* **332** (2007) 709–726.
- [21] P. van den Driessche and J. Watmough, Reproduction numbers and sub-threshold endemic equilibria for compartmental models of disease transmission, *Mathematical Biosciences* **180** (2002) 29–48.
- [22] N. Chitnis, J. M. Hyman and J. M. Cushing, Determining important parameters in the spread of malaria through the sensitivity analysis of a mathematical model, *Bulletin of Mathematical Biology* **70** (2008) 1272–1296.